The Astrophysical Journal Supplement Series, 172:1–8, 2007 September

THE COSMIC EVOLUTION SURVEY (COSMOS): OVERVIEW[1]

N. Scoville,[2,3] H. Aussel,[4] M. Brusa,[5] P. Capak,[2] C. M. Carollo,[6] M. Elvis,[7] M. Giavalisco,[8] L. Guzzo,[9] G. Hasinger,[5] C. Impey,[10] J.-P. Kneib,[11] O. LeFevre,[11] S. J. Lilly,[6] B. Mobasher,[8] A. Renzini,[12,13] R. M. Rich,[14] D. B. Sanders,[15] E. Schinnerer,[16,17] D. Schminovich,[18] P. Shopbell,[2] Y. Taniguchi,[19] and N. D. Tyson[20]

Received 2006 April 25; accepted 2006 June 28

ABSTRACT

The Cosmic Evolution Survey (COSMOS) is designed to probe the correlated evolution of galaxies, star formation, active galactic nuclei (AGNs), and dark matter (DM) with large-scale structure (LSS) over the redshift range $z > 0.5-6$. The survey includes multiwavelength imaging and spectroscopy from X-ray–to–radio wavelengths covering a 2 deg^2 area, including *HST* imaging. Given the very high sensitivity and resolution of these data sets, COSMOS also provides unprecedented samples of objects at high redshift with greatly reduced cosmic variance, compared to earlier surveys. Here we provide a brief overview of the survey strategy, the characteristics of the major COSMOS data sets, and a summary the science goals.

Subject headings: cosmology: observations — dark matter — galaxies: evolution — galaxies: formation — large-scale structure of universe — surveys

1. INTRODUCTION

Our understanding of the formation and evolution of galaxies and their large-scale structures (LSSs) has advanced enormously over the last decade—a result of a phenomenal synergy between theoretical and observational efforts. Deep observational studies using the *Hubble Space Telescope* (*HST*) and the largest ground-based telescopes have probed galaxy and AGN populations back to redshift $z = 6$ when the universe had aged less than 1 billion of its current 13 billion years. Just as remarkable is the enormous success of numerical simulations for ΛCDM models in reproducing many of the current LSS characteristics, all starting from an initial, nearly uniform, hot universe.

The Hubble Deep Fields (HDF-N and HDF-S), GOODS, and UDF have provided exquisite imaging of galaxy populations in narrow cones out to $z \sim 5$–6 (Williams et al. 1996, 2000; Giavalisco et al. 2004; Beckwith et al. 2006). Ground-based multiband imaging and spectroscopy provide redshifts and hence cosmic ages for these populations. Most briefly, the early universe galaxies were more irregular/interacting than at present and the overall cosmic star formation rate probably peaked at $z \sim 1$–3 with 10–30 times the current rates (Lilly et al. 1996; Madau et al. 1996; Chary & Elbaz 2001). Although some large-scale structure and clustering of the luminous, high-redshift galaxies is in evidence (e.g., Ettori et al. 2004; Mei et al. 2006), it is the theoretical simulations that have best characterized (or at least hypothesized) the larger scale, dark matter structure (e.g., Benson et al. 2001; Springel et al. 2005). In fact, the major gap that exists in our current understanding is the coupling between the LSS and the evolution of luminous galaxies—specifically, their assembly via merging and their star formation and AGN fueling, both probably also linked to galactic interactions and mergers (e.g., Hernquist & Springel 2003).

The COSMOS survey is the first survey encompassing a sufficiently large area that it can address the coupled evolution of LSS, galaxies, star formation, and AGNs. COSMOS is the largest

[1] Based on observations with the NASA/ESA *Hubble Space Telescope*, obtained at the Space Telescope Science Institute, which is operated by AURA, Inc., under NASA contract NAS 5-26555; also based on data collected at the Subaru Telescope, which is operated by the National Astronomical Observatory of Japan; the *XMM-Newton*, an ESA science mission with instruments and contributions directly funded by ESA Member States and NASA; the European Southern Observatory under Large Program 175.A-0839, Chile; Kitt Peak National Observatory, Cerro Tololo Inter-American Observatory, and the National Optical Astronomy Observatory, which are operated by the AURA, Inc., under cooperative agreement with the National Science Foundation; the National Radio Astronomy Observatory, which is a facility of the National Science Foundation operated under cooperative agreement by Associated Universities, Inc.; and the Canada-France-Hawaii Telescope with MegaPrime/MegaCam operated as a joint project by the CFHT Corporation, CEA/DAPNIA, the NRC and CADC of Canada, the CNRS of France, TERAPIX, and the University of Hawaii.

[2] California Institute of Technology, MC 105-24, 1200 East California Boulevard, Pasadena, CA 91125.

[3] Visiting Astronomer, University Hawaii, 2680 Woodlawn Drive, Honolulu, HI 96822.

[4] Service d'Astrophysique, CEA/Saclay, 91191 Gif-sur-Yvette, France.

[5] Max-Planck-Institut für Extraterrestrische Physik, D-85478 Garching, Germany.

[6] Department of Physics, ETH Zurich, CH-8093 Zurich, Switzerland.

[7] Harvard-Smithsonian Center for Astrophysics, 60 Garden Street, Cambridge, MA 02138.

[8] Space Telescope Science Institute, 3700 San Martin Drive, Baltimore, MD 21218.

[9] INAF-Osservatorio Astronomico di Brera, via Bianchi 46, I-23807 Merate (LC), Italy.

[10] Steward Observatory, University of Arizona, 933 North Cherry Avenue, Tucson, AZ 85721.

[11] Laboratoire d'Astrophysique de Marseille, BP 8, Traverse du Siphon, 13376 Marseille Cedex 12, France.

[12] European Southern Observatory, Karl-Schwarzschild-Strasse 2, D-85748 Garching, Germany.

[13] Dipartimento di Astronomia, Universita di Padova, Vicolo dell'Osservatorio 2, I-35122 Padua, Italy.

[14] Department of Physics and Astronomy, University of California, Los Angeles, CA 90095.

[15] Institute for Astronomy, 2680 Woodlawn Drive, University of Hawaii, Honolulu, HI 96822.

[16] National Radio Astronomy Observatory, P.O. Box O, Socorro, NM 87801-0387.

[17] Max-Planck-Institut für Astronomie, Königstuhl 17, D-69117 Heidelberg, Germany.

[18] Department of Astronomy, Columbia University, MC2457, 550 West 120th Street, New York, NY 10027.

[19] Astronomical Institute, Graduate School of Science, Tohoku University, Aramaki, Aoba, Sendai 980-8578, Japan.

[20] American Museum of Natural History, Central Park West at 79th Street, New York, NY 10024.

TABLE 1
Expected Numbers of Objects in COSMOS 2 Square Degree Field

Class	Number	I_{AB} (10 σ)	Reference
Galaxies	3.0×10^6	<27.5	COSMOS Subaru: Taniguchi et al. (2007)
Galaxies	1.9×10^6	<27	COSMOS *HST*: Scoville et al. (2007a)
Galaxies	300000	<25	COSMOS: Scoville et al. (2007a); Taniguchi et al. (2007)
XMM-Newton AGNs	~2000	5×10^{-16} cgs	COSMOS *XMM-Newton*: Hasinger et al. (2007); Cappelluti et al. (2007)
XMM-Newton clusters	~120	1×10^{-15} cgs	COSMOS *XMM-Newton*: Finoguenov et al. (2007)
Strong lens systems	60–80		Fassnacht et al. (2004)
Galaxies with spectra	$\sim 5 \times 10^4$	$I \leq 25$	zCOSMOS: Lilly et al. (2006)
QSOs	600 (100)	24 (21)	Croom et al. (2001)
$z > 4$ QSOs	50	25	Cristiani et al. (2004)
ULIRGs	3000	26	Smail et al. (2002)
Extremely red objects	25000	25	Daddi et al. (2000); Smith (2002)
Lyman-break galaxies ($z \leq 2$)	65000	25.5	Steidel et al. (2004)
Lyman-break galaxies ($z \sim 3$)	10000	25.5	Shapley et al. (2001)
Red high-z galaxies ($z > 2$)	10000	25.5	Labbé et al. (2003)
L,T dwarfs	300 (<200 pc)	28 (4 σ)	Burgasser et al. (2002)
Kuiper Belt objects	100–250	27	S-COSMOS: Sanders et al. (2007)

HST survey ever undertaken—imaging an equatorial, ~2 deg^2 field with single-orbit *I*-band exposures to a point source depth of $I_{AB} = 28$ mag and 50% completeness for galaxies 0.5″ in diameter at $I_{AB} = 26.0$ mag (5 σ, Scoville et al. 2007a). Extensive multiwavelength ground- and space-based observations of this field (see § 4) have been gathered or are anticipated, spanning the entire spectrum from X-ray, UV, optical/IR, mid-infrared, mm/submillimeter, and to radio with extremely high-sensitivity imaging and spectroscopy (Hasinger et al. 2007; Taniguchi et al. 2007; Capak et al. 2007a; Lilly et al. 2006; Sanders et al. 2007; Bertoldi et al. 2007; Schinnerer et al. 2007). This full spectrum approach is required to probe the coupled evolution of young and old stellar populations, starbursts, the ISM (molecular and ionized components), AGNs, and dark matter. The multiwavelength approach is also necessitated by the fact that light from different cosmic epochs is differentially redshifted and the presence of dust obscuration in many of the most rapidly evolving galactic regions. The large areal coverage of COSMOS is motivated to sample the largest structures existing in the local universe since smaller area coverage leads to severe cosmic variance.

COSMOS will detect $\simeq 2 \times 10^6$ galaxies and AGNs (see Table 1), sampling a volume in the high-redshift universe approaching that sampled locally by the Sloan Digital Sky Survey (SDSS). In this article, we provide a brief overview of the scientific goals of the COSMOS survey and an overall summary of the survey observational program, providing an introduction to the subsequent articles in this Supplement, which provide more detailed description of the separate observational programs and the initial science results, based on the first 2 years of the survey.

2. COSMOS SCIENCE GOALS

The COSMOS survey addresses nearly every aspect of observational cosmology over the majority of the Hubble time, out to $z \sim 6$:

1. the assembly of galaxies, clusters, and dark matter on scales up to $\geq 2 \times 10^{14}\ M_\odot$;
2. reconstruction of the dark matter distributions and content using weak gravitational lensing at $z < 1.5$;
3. the evolution of galaxy morphology, galactic merger rates, and star formation as a function of LSS environment and redshift;
4. evolution of AGNs and the dependence of black hole growth on galaxy morphology and environment;
5. the mass and luminosity distribution of the earliest galaxies, AGNs, and intergalactic gas at $z = 3$–6 and their clustering.

The growth of galaxies, AGNs, and dark matter structure is traced in COSMOS over a period corresponding to ~75% of the age of the universe. For reference, we show in Figure 1 the comoving volume and differential volumes sampled by COSMOS as a function of z, together with the age and look-back times. The largest survey of the local universe (SDSS) samples approximately $3 \times 10^7\ h^{-3}$ Mpc^3 at $z \leq 0.1$ (SDSS Web page); COSMOS samples equivalent or larger volumes in the early universe (see Fig. 1).

The expected numbers of different types of objects in the 2 deg^2 field at the COSMOS sensitivities are given in Table 1. Over 2 million galaxies are detected in the *HST* ACS and Subaru optical imaging and photometric redshifts have been determined for approximately 800,000 galaxies (Mobasher et al. 2007). The COSMOS spectroscopic surveys (VLT and Magellan; Lilly et al. 2006) will yield ~40,000 galaxies with accurate redshifts at $z =$ 0.5–2.5, all having 0.05″ *HST* imaging. Redshift bins can then be constructed, each with thousands of galaxies, to probe evolution of the morphological distribution (E, Sp, Irr, etc.) as a function of both LSS and time. Each redshift slice of width $\Delta z \simeq 0.02$ (fine enough to resolve structures along the line of sight; see Fig. 2) will have 500–1000 galaxies. Evolution of the luminosity and spatial correlation functions for type-selected galaxies can be analyzed with unprecedented statistical accuracy.

2.1. *Large-Scale Structure*

Figure 2 shows the results of a LSS Λ-CDM simulation for $z = 1$ and 2 (Virgo Consortium; Frenk et al. 2000). The gray scale shows the dark matter distributions, and the dots represent galaxies chosen by semianalytic techniques to populate the DM halos. Observational studies of Lyman-break galaxies and deep X-ray imaging with *Chandra*/*XMM-Newton* are broadly consistent with these models with respect to the LSS (Giavalisco et al. 1998; Adelberger et al. 1998; Gilli et al. 2003).

The need to sample very large scales arises from the fact that structure occurs on mass scales up to $\geq 10^{14}\ M_\odot$ and existing smaller, contiguous surveys (see Fig. 2) are likely to be unrepresentative at $z \sim 1$. This is illustrated in Figure 3, which shows the probability of enclosing a given mass as a function of field size. Earlier projects, such as GOODS (Giavalisco et al.

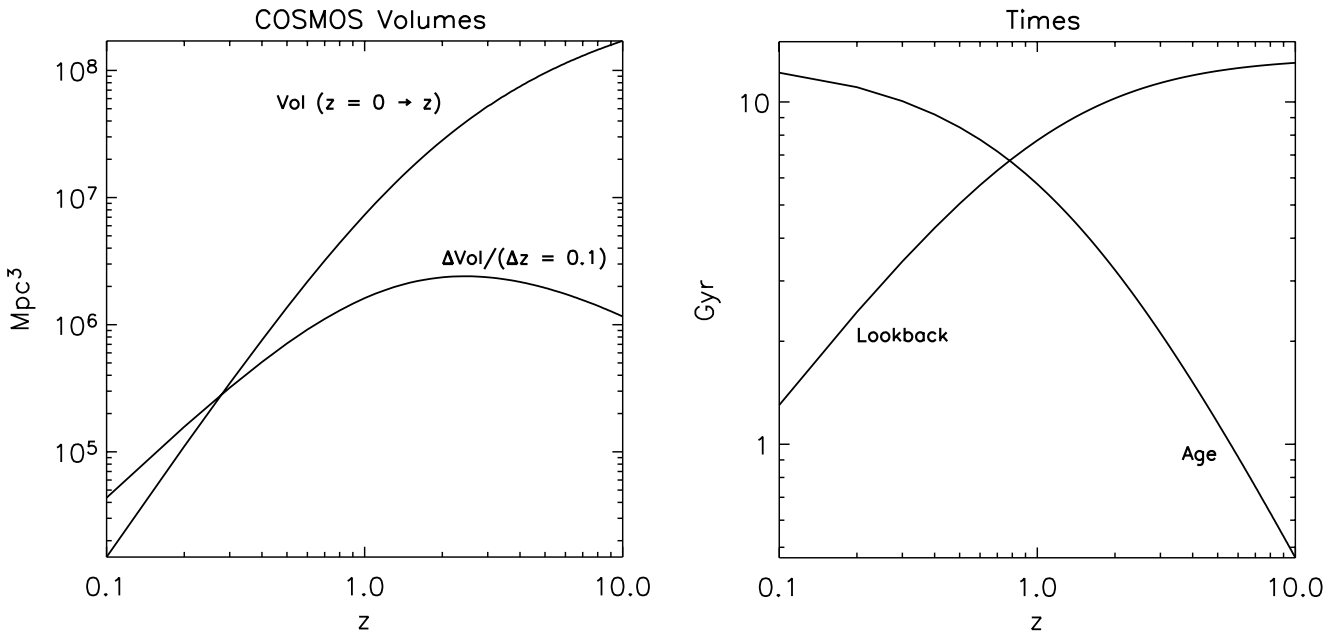

FIG. 1.—*Left*: Volumes sampled by COSMOS out to redshift z and in a shell of width $\Delta z = 0.1$ for a nominal area of 2 deg^2. (The COSMOS ACS imaging covers $\sim$1.8, whereas the ground-based photometry is complete in most bands over $\sim$2.55 deg^2.) *Right*: Cosmic age and look-back times as a function of z for the concordance model ($H_0 = 70$ km s^{-1} Mpc^{-1}, $\Omega_m = 0.3$, and $\Omega_\Lambda = 0.7$).

2004) and GEMS (Rix et al. 2004), adequately sample masses up to $3 \times 10^{13}\ M_\odot$, whereas COSMOS samples the largest expected structures at $\sim 2 \times 10^{14}\ M_\odot$ (dark and luminous matter). The evolution of the halo and cluster mass distribution is shown in the right panel of Figure 3—dramatically demonstrating the evolution of the dark matter on scales probed by COSMOS. Evolution of the luminous-galaxy occupation number in halos as a function of both redshift and halo mass can provide stringent tests of LSS models. COSMOS yields critical data on the efficiency of star formation as a function of environment and cosmic epoch.

2.2. *Gravitational Lensing and Dark Matter*

The small distortions to the shapes of background galaxies resulting from weak gravitational lensing by foreground structures depend on the distribution of dark matter as characterized by the evolution of its power spectrum $P(k, z)$ (Kaiser et al. 1995;

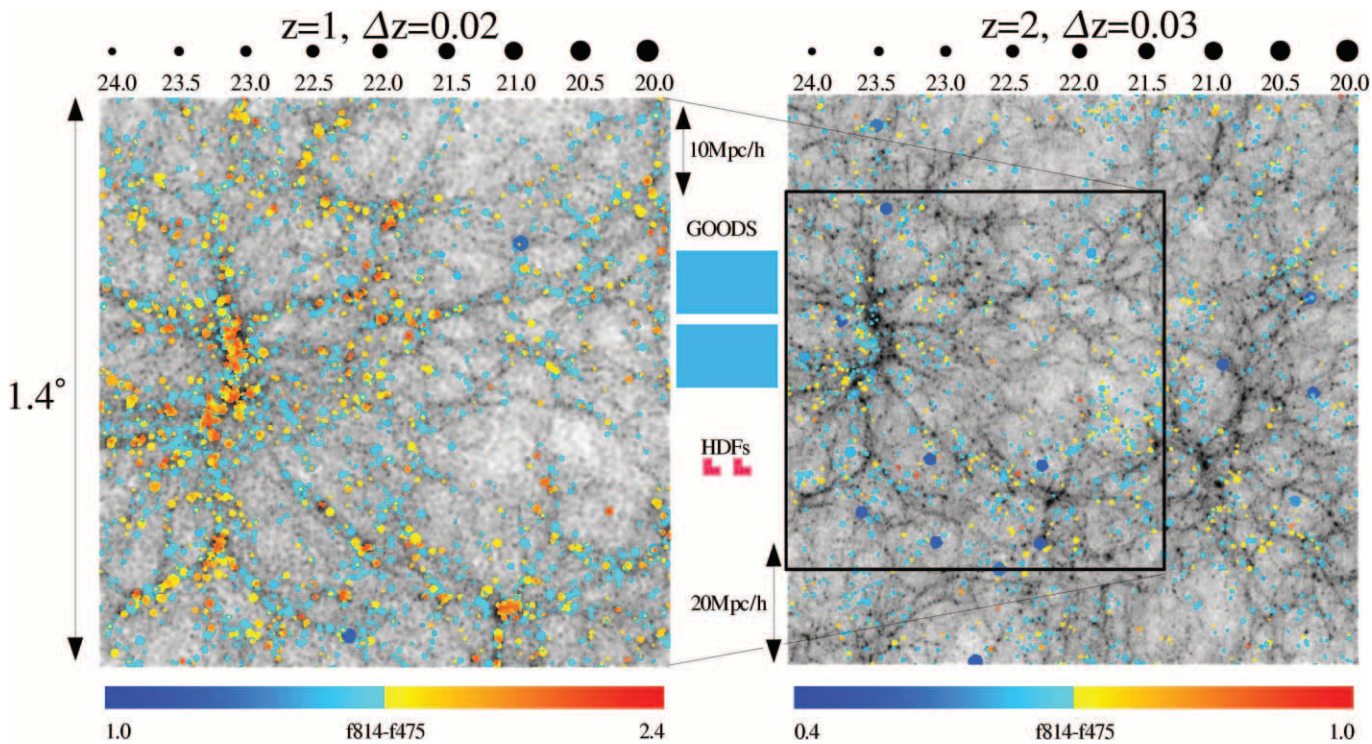

FIG. 2.—ΛCDM simulation results for 2 deg^2 at $z = 1$ and 2, illustrating the scales of voids and wall regions and the "expected" correlation of galaxy evolution with environmental density (Frenk et al. 2000). The gray scale indicates the dark matter distribution and the symbols show magnitudes of galaxies computed for the *I* band. The depth of the redshift slice is $\Delta z = 0.02$ (50 Mpc at $z = 1$). Also shown are the HDF and GOODS field sizes; the GEMS field size is 1/4 deg^2.

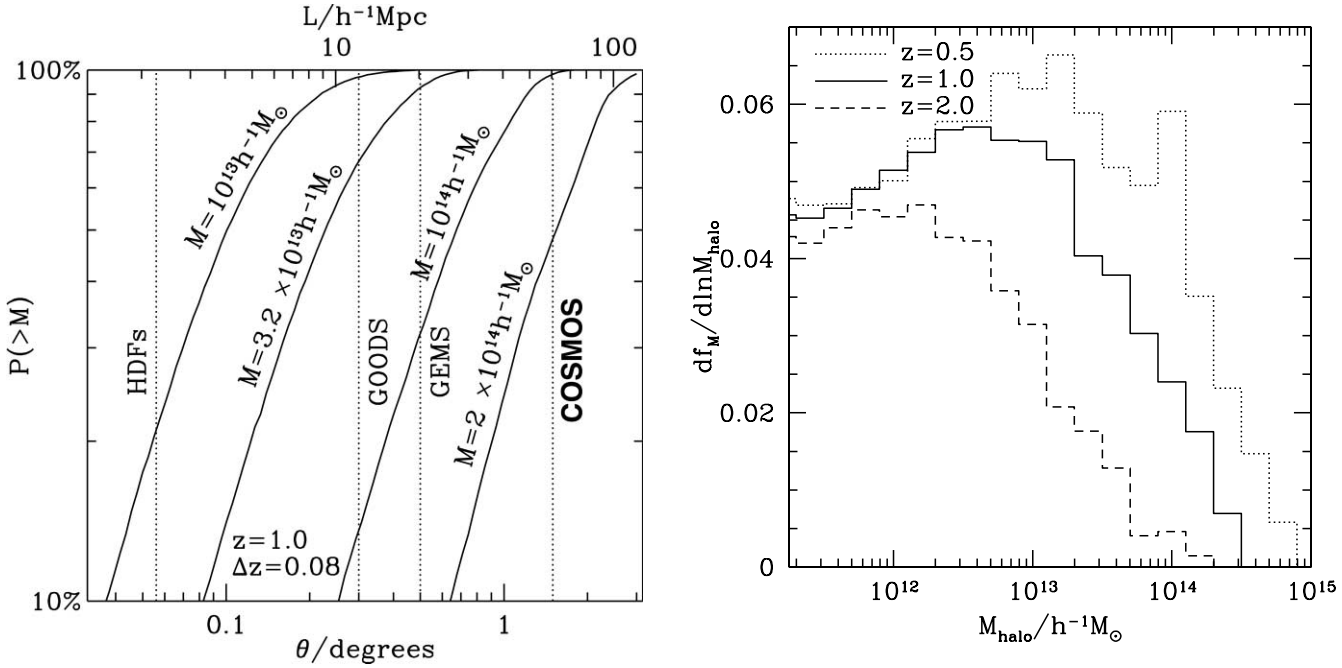

FIG. 3.—*Left*: Probability of enclosing at least one structure of the specified mass is shown as a function of the field size at $z = 1$ from the Virgo consortium ΛCDM simulation (Frenk et al. 2000). The masses shown correspond approximately to the Local group, a "poor" cluster, Virgo and about 30% of Coma. *Right*: Distribution of halo masses is shown for $z = 0.5$, 1, and 2, illustrating the expected (but not yet verified) evolution in the halo and cluster mass distributions from the ΛCDM simulation (Frenk et al. 2000). $\Delta z \simeq 0.08$ was chosen only to have a significant probability of including a massive structures, but $\Delta z \simeq 0.02$ is required to resolve structures in the line of sight.

Mellier 1999; Refregier 2003). The reliability of the derived results depends on the dispersion of the intrinsic shapes of the background sources, instrumental PSFs, and the number of background, lensed galaxies and their redshifts. The ACS PSF permits extraction of shapes for ∼87 galaxies per arcmin^2, 2–3 times more than the number in the best ground-based data (Park et al. 2004; Rhodes et al. 2007). Resulting dark matter maps thus have much higher fidelity and improved sensitivity (down to $10^{13}\,M_\odot$). The observed distributions of halo masses can then be compared with the theoretically predicted evolution as a function of redshift over the range 10^{13} to $2 \times 10^{14}\,M_\odot$ (Bahcall et al. 2004).

2.3. *Assembly and Evolution of Galaxies*

Galaxies in the early universe are built up by two major processes: dissipative collapse and merging of lower mass protogalactic and galactic components. Their intrinsic evolution is then driven by the conversion of primordial and interstellar gas into stars, with galactic merging and interactions triggering star formation and starbursts. While there is general agreement over this qualitative picture, the precise timing of these events, as well as their relation to local environment, remains to be observationally explored. For example, the assembly of massive galaxies apparently takes place at substantially earlier epochs ($z > 2$) than predicted in the earlier semianalytic models. Spheroids include the majority of the stellar mass in the local universe (Fukugita et al. 1998) and may have formed at very early times ($z >$ 2–3; Renzini 2006; Peebles 2002; Bell et al. 2004). Their progenitors at $z \sim 3$ are possibly detected as Lyman-break galaxies (Adelberger et al. 2005) and/or SCUBA sources (Eales et al. 1999; Blain et al. 2004). The Gemini Deep Deep Survey (Glazebrook et al. 2004) and K20 Survey (Cimatti et al. 2004) find massive, passively evolving galaxies out to $z \sim 2$; The Gemini Deep Survey finds massive galaxies out to $z \sim 2$; HDF-N has few massive galaxies and those in the HDF-S are at higher z, suggesting strong environmental dependence and underscoring the need for large fields. As for spiral galaxies, their major epoch of formation may be in the range $z =$ 1–2 (Ferguson et al. 2000; Conselice et al. 2004).

3. COSMOS FIELD SELECTION

The COSMOS field is located near the celestial equator to ensure visibility by all astronomical facilities, especially unique instruments such as the next generation 20–30 m optical/IR telescope(s). The time requirements for deep imaging and spectroscopy over a total area of 2 deg^2, containing over a million galaxies makes it strategically imperative that the field be readily observable by all large optical/IR telescopes. For radio studies, high-declination fields such as Lockman Hole, HDF-N, Groth strip, and CDF-S are ruled out—they cannot be easily observed by *both* (E)VLA in the north and ALMA in the south.

The COSMOS field is a $1.4^\circ \times 1.4^\circ$ square, aligned east-west, north-south, centered at R.A. $= 10^{\rm h}00^{\rm m}28.6^{\rm s}$, decl. $= +02^\circ12'21.0''$ (J2000.0). (The field is near to, but offset from, the R.A. = 10 hr VVDS field.) The field is devoid of bright X-ray, UV, and radio sources. Relative to other equatorial fields, COSMOS has exceptionally *low and uniform Galactic extinction* ($\langle E_{(B-V)} \rangle \simeq 0.02$ mag).

3.1. *IR Backgrounds*

The most serious concern for equatorial, survey fields is that they have somewhat higher IR backgrounds than the most favorable high Galactic and ecliptic latitude fields. In Table 2, we tabulate the backgrounds and comparative sensitivities (5 σ) for COSMOS, SWIRE *XMM-Newton* (another equatorial field), and the lowest background, high-declination fields such as Lockman Hole, CDF-S, HDF-N, and Groth Strip (which all have similar backgrounds). For the COSMOS field, we use the background appropriate to the time when it is observed by *Spitzer*; for the other fields we have use their minimum background estimates. For the

TABLE 2
INFRARED BACKGROUNDS AND SENSITIVITIES (1600 s)

FIELD	8 μm Background (MJy sr^{-1})	8 μm S_ν (5 σ) (μJy)	24 μm Background (MJy sr^{-1})	24 μm S_ν (5 σ) (mJy)	100 μm BACKGROUND (MJy sr^{-1})
COSMOS	6.9	12.7	37	0.080	0.90
Lockman, CDF-S	5.0–5.3	11.0	18.4–19.4	0.061	0.45
SWIRE-*XMM-Newton*	7.1	12.9	31.1	0.078	1.25

NOTES.—Background estimates obtained using the *Spitzer* Science Center (SSC) Spot program. Sensitivity estimates for 1600 s of integration obtained using the SSC Sens-Pet program and interpolating to the specified background level, scaling as the square root of the background.

COSMOS field, the mean 100 μm background is 0.90 MJy sr^{-1}, compared to $\sim$0.45 MJy sr^{-1} in the very best, nonequatorial fields such as Lockman Hole. However, the sensitivity for a given integration time, scales as the square root of the background emission. Therefore, the lowest background fields (Lockman Hole, CDF-S, HDF-N, and Groth Strip) will have only $\sim$15%–25% better sensitivity than COSMOS for equivalent integration times (Table 2). This small reduction in sensitivity, associated with selection of an equatorial field, was deemed an acceptable compromise when weighed against the inaccessibility of higher declination fields to the unique ground-based facilities.

4. COSMOS MULTIWAVELENGTH SURVEYS

The COSMOS field is accessible to essentially all astronomical facilities, enabling complete multiwavelength data sets (X-ray, UV, optical/IR, FIR/submillimeter to radio). The status of these observational programs is summarized in Table 3, and on the COSMOS Web site.[21] The extensive allocations on Subaru, CFHT, UKIRT, and NOAO have providing extremely deep photometry for 12 bands from U to K_s, enabling accurate photoredshifts, integrated colors, and color selection of populations (e.g., LBGs, EROs, AGNs, etc.) for essentially all objects detected in the 2 deg^2 ACS field. The photometry catalogs from these data contain over 2 million objects at $<$27 mag (AB) in the U to K_s bands. The initial photometric redshift catalog has 860,000 objects at $<$25 mag (i-band) (Mobasher et al. 2007). The ground-based imaging is an on-going effort, currently directed toward obtaining narrow- and intermediate-width filter imaging with

[21] See http://www.astro.caltech.edu/~cosmos/.

TABLE 3
MULTIWAVELENGTH COSMOS DATA

Data	Bands/λ/Res.	Number of Objects	Sensitivity[a]	Investigators	Time
HST ACS	814I		28.8	Scoville et al.	581 orbits
	475g		28.15	Scoville et al.	9 orbits
HST NIC3	160W		25.6 (6% area)	Scoville et al.	590 orbits
HST WFPC2	300W		25.4	Scoville et al.	590 orbits
Subaru SCam	B, V, r', i, z', g'		28–26	Taniguchi et al.	10 n
	10 IB filters		26	Taniguchi, Scoville	11 n
	NB816		25	Taniguchi et al.	8 n
CFHT Megacam	u^*		27	Sanders et al.	24 hr
	u, i^*		26	LeFevre et al.	12 hr
CFHT LS	u–z			Deep LS Survey	
NOAO CTIO	K_s		21	Mobasher et al.	18 n
CFHT UKIRT	J, H, K		24.5–23.5	Sanders et al.	12 n
UH-88	J		21	Sanders et al.	10 n
GALEX	FUV, NUV		26.1, 25.8	Schminovich et al.	200 ks
XMM-Newton EPIC	0.5–10 keV		10^{-15} cgs	Hasinger et al.	1.4 Ms
Chandra	0.5–7 keV			Elvis et al.	Future
VLT VIMOS sp.	R = 200	3000	$I < 23$	Kneib et al.	20 hr
	R = 600	20000	$I < 22.5$, $0.1 \leq z \geq 1.2$	Lilly et al.	600 hr
	R = 200	10000	$B < 25$, $1.4 \leq z \geq 3.0$	Lilly et al.	600 hr
Mag. IMAX sp.	R = 3000	2000		Impey, McCarthy, Elvis	12 n
Keck GEMINI sp.	R = 5000	4000	$I < 24$	Team Members	
Spitzer MIPS	160, 70, 24 μm		17, 1, 0.15 mJy	Sanders et al.	392 hr
Spitzer IRAC	8, 6, 4.5, 3 μm		11,9,3,2 μJy	Sanders et al.	220 hr
IRAM MAMBO	1.2 mm		1 mJy (20 $\times$ 20$'$)	Bertoldi et al.	90 hr
CSO Bolocam	1.1 mm		3 mJy	Aquirre et al.	40 n
JCMT Aztec	1.1 mm		0.9 mJy (1 σ)	Sanders et al.	5 n
VLA A	20 cm		7 μJy (1 σ)	Schinnerer et al.	60 hr
VLA A/C	20 cm		10 μJy (1 σ)	Schinnerer et al.	275 hr
SZA (full field)	9 mm		S–Z to 2 $\times$ 10^{14} $M_\odot$	Carlstrom et al.	2 mth

[a] Sensitivities are AB mag and 5 σ for a point source unless noted otherwise.

Subaru SuprimeCam (for more accurate redshifts and detection of high-z emission-line objects) and deeper near-infrared imaging at UKIRT, CFHT, and UH88.

A very large VLT/VIMOS program (zCOSMOS) will provide spectra and redshifts for $\geq$30,000 galaxies up to $z \sim 3$ (Lilly et al. 2006). A second spectroscopy program, focussed toward the AGN population and red objects, is being conducted on Magellan/IMACS. The VLT and Magellan spectroscopy is expected to complete within $\sim$3 yr.

XMM-Newton has devoted 1.4 Ms to a complete X-ray survey of the field (Hasinger et al. 2007), and COSMOS was one of the deep *GALEX* fields for UV imaging (Zamojski et al. 2007). The VLA-COSMOS survey was allocated 275(+60) hr for the largest deep wide field image ever done at arcsec resolution (Schinnerer et al. 2007). The *XMM-Newton*, *GALEX*, and VLA surveys are all now complete. Deep mid-infrared observations (IRAC) and shallower far-infrared observations (MIPS) of the full COSMOS field have been obtained with *Spitzer* (see Table 3; Sanders et al. 2007). At mm/submillimeter-wavelengths, partial surveys of COSMOS are on-going at the IRAM 30 m and CSO telescopes (Bertoldi et al. 2007; J. Aguirre et al. 2007, in preparation).

5. MAJOR OBSERVATIONAL GOALS

In this section, we briefly review the major ingredients of the COSMOS survey.

5.1. *Galaxy Redshifts: Photometric and Spectroscopic*

Determining the redshifts or look-back time of individual galaxies is clearly one of the most difficult and time-consuming aspects of any cosmological evolution survey. In COSMOS this is even more difficult since the redshifts are needed with sufficient precision not just to determine the cosmic epoch, but also to place the galaxies within (or outside) structures along the line of sight. Without high precision, structures become "blurred" due to the scattering of galaxies to different distances in the line of sight, and for specific galaxies, their environment cannot be determined. The accuracy of redshifts required for the environmental specification is $\Delta z/(1+z) \leq 0.02$ based on LSS simulations such as shown in Figure 2; lower precision degrades the LSS/environmental definition.

In COSMOS, photometric redshifts (Mobasher et al. 2007) are obtained from deep (mostly ground-based) imaging—from Subaru (Taniguchi et al. 2007), CFHT, UKIRT, and NOAO (Capak et al. 2007a). At present the photometric-redshift accuracy is $\sigma_z/(1+z) \sim 0.04$ for approximately 2×10^5 galaxies at $z < 1.2$ (and 0.1 accuracy for 8×10^5 galaxies), enabling initial definition of the LSS, especially for the denser environments (Scoville et al. 2007b; Finoguenov et al. 2007). Expected improvements in the sensitivity of the near-infrared imaging and the addition of more bands should further increase the accuracy and increase the redshift range of the photometric redshifts within the next year.

Very large spectroscopic surveys are now ongoing as part of COSMOS at the VLT and Magellan telescopes (Lilly et al. 2006). The spectroscopic sample will eventually include approximately 37,500 galaxies and several thousand AGNs down to limits of $I_{\rm AB} = 24.5$. The zCOSMOS spectroscopy provides precision of $\sim$0.0003 in redshift for the brighter objects at $z < 1.2$ and somewhat lower precision for the fainter objects. These spectroscopic samples will provide very precise definition of the environment, albeit for smaller subsets of the overall COSMOS galaxy population.

5.2. *Galaxy Evolution: HST Imaging and SEDs*

The evolutionary status of galaxies can be analyzed from either their morphologies or their spectral energy distributions (SEDs, characterizing the stellar population).

Morphological parameters for the galaxies are obtained from the *HST* imaging (e.g., bulge/disk ratios, concentration, asymmetry, size, multiplicity, clumpiness; Scarlata et al. 2007; Cassata et al. 2007; Capak et al. 2007b). The COSMOS *I*-band ACS images have sufficient depth and resolution to allow classical bulge-disk decomposition for L^* galaxies at $z \leq 2$, while less detailed structural parameters such as compactness, asymmetry, clumpiness and size can be measured for all galaxies down to the spectroscopic limit ($I_{\rm AB} \sim 25$), out to $z \sim 5$. None of these measures can be obtained from ground-based imaging at these flux levels; ACS imaging has been a critical ingredient for understanding the evolution and build-up of galaxies.

In COSMOS, deep imaging (from Subaru, *GALEX*, UKIRT and NOAO, and *Spitzer* IRAC) provides SEDs to characterize the integrated stellar populations of the 1–2 million galaxies detected with *HST*. The rest-frame SEDs are derived self-consistently with the photometric redshift determinations. (For most of the galaxies, the multicolor imaging has insufficient resolution to measure internal population or extinction gradients.)

5.3. *Environment: Galaxy Overdensities, DM Weak Lensing, and Correlation Functions*

The environment or LSS in which a given galaxy resides might be defined from the local number density of galaxies or from the DM density as determined from weak lensing or the galaxy-galaxy velocity dispersion. The COSMOS *HST* imaging provides measures of the close-in environment (from galaxy multiplicity and merger indicators such as tidal distortions) and larger scale DM environment (from weak lensing shear analysis; Massey et al. 2006). As noted in § 5.1, definition of the environment is critically dependent on moderately high-accuracy spectroscopic (or photometric) redshifts; the integrated, multiwavelength approach adopted for COSMOS is intended to maximize the impact and utility of each component. Having multiple approaches to environmental determination will provide added confidence in the LSS definition. An example of this is the use of diffuse X-ray emission as detected in the COSMOS *XMM-Newton* survey to identify and confirm galaxy groups and clusters (Finoguenov et al. 2007).

The wide-area, uniform ACS, and Subaru COSMOS surveys allow determination of spatial correlation functions as a function of type (morphological and SED) and luminosity and their evolution with redshift and environment. The enormous sizes of the samples that become available in COSMOS enable precision approaching that of SDSS but at much higher redshift. Clustering of different populations of galaxies, probed by the correlation function, is related to the distribution of underlying dark matter from weak lensing. COSMOS provides over a hundred slices of the universe back to $z \sim 2$ to reveal the spatial distribution and shapes of tens of thousands of galaxies sampling the full range of cosmic structure.

5.4. *Activity: Starbursts and AGNs*

The COSMOS survey samples $\sim$45,000 galaxies spectroscopically—providing an enormous sample of emission line tracers of both starbursts and AGNs over a broad range of redshift. In addition, complete very high sensitivity radio continuum (VLA; Schinnerer et al. 2007) and X-ray (*XMM-Newton*;

TABLE 4
COSMOS Data Archives and Web sites

Location	Contents	URL
COSMOS Web site	Project and science Web pages + links	http://www.astro.caltech.edu/~cosmos/
COSMOS archive (IPAC/IRSA)	Imaging: *HST*, Subaru, NOAO, CFHT, UH, UKIRT, *XMM-Newton*, VLA, *GALEX*; Spectroscopy: VLT-VIMOS, Mag.-IMAX	http://irsa.ipac.caltech.edu/data/COSMOS/
STScI MAST	Imaging: *HST*	http://archive.stsci.edu/
INAF - IASF Milano	Data tools and archive	http://cosmosdb.mi.iasf.cnr.it
Obs. Marseille	Spectroscopy archive	http://cencosw.oamp.fr/EN/index.en.html

Hasinger et al. 2007) coverage directly probes the population of AGNs; the radio continuum sensitivity allows the detection of the very luminous starburst populations out to a redshift of $\sim$1.5 and the most luminous systems out to $z \sim 3$. Less luminous radio galaxies (type FRI) could be seen out to $z \sim 5$. Coverage with *Spitzer* MIPS detects dust-embedded ultraluminous starbursts and AGNs out to $z \sim 2$–3 (Sanders et al. 2007). COSMOS includes large samples of galaxies with multiple, independent tracers of luminous activity. These can be analyzed as a function of both redshift and environment, opening up fundamental investigations of starburst and AGN fueling in the early universe. Millimeter/submillimeter–wavelength surveys of the COSMOS field have been initiated to identify the most luminous starbursts at $z > 1$ (Bertoldi et al. 2007; J. Aguirre et al. 2007, in preparation). In the long term, high-resolution imaging with ALMA will be a vital capability—providing resolved images of the neutral ISM, luminosity distribution, and dynamical masses for virtually all COSMOS galaxies having ISMs equivalent to the Galaxy. The COSMOS field was specifically selected to ensure ALMA access (see § 3).

5.5. $z = 3$–6: *High-Redshift Galaxies, LSS, and IGM*

The large areal coverage and high sensitivity of the COSMOS survey provides significant samples of $z > 3$ objects, selected by multiband color criteria, the Lyman-break method, or by direct detection of Lyα emission lines (Murayama et al. 2007). At these higher redshifts, the field subtends over 200 Mpc (comoving) and samples a volume similar to that sampled locally by SDSS.

6. COSMOS DATA ARCHIVES AND WEB SITES

Table 4 list URLs for the COSMOS survey. The major COSMOS data sets become publicly available in staged releases (following calibration and validation) through the IPAC/IRSA Web site.[22] The COSMOS *HST* data are also available at STScI-MAST.[23] Archives are also maintained at INAF-IASF[24] and Obseratoire de Marseille[25] in Europe. These archives include calibrated image and spectral data and catalogs when they are each released (typically 1 yr after acquisition).

7. SUMMARY

The long-term legacy of COSMOS: COSMOS is the largest contiguous area ever imaged by *HST*. It is likely to remain for the next decades the largest area imaged in the optical at better than 0.05″ resolution, well through the *JWST* era. As such, it is destined to represent the reference field for future studies of observational cosmology, attracting massive time investments by every new facility coming on line, e.g., ALMA, *Herschel*, *JWST*, etc. While we have expanded on several immediate scientific goals of the project, we believe that the long-term legacy of COSMOS will allow scientific applications well beyond those listed in the present paper.

We gratefully acknowledge the contributions of the entire COSMOS collaboration consisting of more than 70 scientists. The *HST* COSMOS Treasury program was supported through NASA grant HST-GO-09822. The COSMOS Science meeting in 2005 May was supported in part by the NSF through grant OISE-0456439.

Facilities: HST (ACS), HST (NICMOS), HST (WFPC2), Subaru (Scam), NRAO (VLA), XMM, GALEX, Spitzer (IRAC), Spitzer (MIPS), CFHT, UKIRT, CSO, IRAM (30m).

[22] See http://irsa.ipac.caltech.edu/data/COSMOS/.
[23] See http://archive.stsci.edu/.
[24] See http://cosmosdb.mi.iasf.cnr.it.
[25] See http://cencosw.oamp.fr/EN/index.en.html.

REFERENCES

Adelberger, K., Steidel, C. C., Giavalisco, M., Dickinson, M., Pettini, M., & Kellogg, M. 1998, ApJ, 505, 18
Adelberger, K., Steidel, C. C., Pettini, M., Shapley, A. E., Reddy, N. A., & Erb, D. K. 2005, ApJ, 619, 697
Bahcall, N., Hao, L., Bode, P., & Dong, F. 2004, ApJ, 603, 1
Bell, E., et al. 2004, ApJ, 608, 752
Beckwith, S. V. W., et al. 2006, AJ, 132, 1729
Benson, A. J., Frenk, C. S., Baugh, C. M., Cole, S., & Lacey, C. G. 2001, MNRAS, 327, 1041
Bertoldi, F., et al. 2007, ApJS, 172, 132
Blain, A. W., Chapman, S. C., Smail, I., & Ivison, R. 2004, ApJ, 611, 725
Burgasser, A., et al. 2002, ApJ, 564, 421
Capak, P., et al. 2007a, ApJS, 172, 284
———. 2007b, ApJS, 172, 99
Cappellutti, N., et al. 2007, ApJS, 172, 341
Cassata, P., et al. 2007, ApJS, 172, 270
Chary, R., & Elbaz, D. 2001, ApJ, 556, 562
Conselice, C., et al. 2004, ApJ, 600, L139
Cristiani, S., et al. 2004, ApJ, 600, L119
Croom, S. M., Warren, S. J., & Glazebrook, K. 2001, MNRAS, 328, 150
Daddi, E., Cimatti, A., Pozzetti, L., Hoekstra, H., Röttgering, H. J. A., Renzini, A., Zamorani, G., & Mannucci, F. 2000, A&A, 361, 535
Eales, S., Lilly, S., Gear, W., Dunne, L., Bond, J. R., Hammer, F., Le Fèvre, O., & Crampton, D. 1999, ApJ, 515, 518
Ettori, S., Tozzi, P., Borgani, S., & Rosati, P. 2004, A&A, 417, 13
Fassnacht, C., Moustakas, L. A., Casertano, S., Ferguson, H. C., Lucas, R. A., & Park, Y. 2004, ApJ, 600, L155
Ferguson, H. C., Dickinson, M., & Williams, R. 2000, ARA&A, 38, 667
Finoguenov, A., et al. 2007, ApJS, 172, 182
Frenk, C., et al. 2000, preprint (astro-ph/0007362)
Fukugita, M., Hogan, C. J., & Peebles, P. J. E. 1998, ApJ, 503, 518
Giavalisco, M., Steidel, C. C., Adelberger, K. L., Dickinson, M. E., Pettini, M., & Kellogg, M. 1998, ApJ, 503, 543
Giavalisco, M., et al. 2004, ApJ, 600, L103
Gilli, B., et al. 2003, ApJ, 592, 721
Glazebrook, K., et al. 2004, Nature, 430, 181
Hasinger, G., et al. 2007, ApJS, 172, 29
Hernquist, L., & Springel, V. 2003, MNRAS, 341, 1253

Kaiser, N., Squires, G., & Broadhurst, T. 1995, ApJ, 449, 460
Labbé, I., et al. 2003, AJ, 125, 1107
Lilly, S. J., Le Fevre, O., Hammer, F., & Crampton, D. 1996, ApJ, 460, L1
Lilly, S., et al. 2006, ApJS, 172, 70
Madau, P., Ferguson, H. C., Dickinson, M. E., Giavalisco, M.,,Steidel, C. C., & Fruchter, A. 1996, MNRAS, 283, 1388
Massey, R. J., et al. 2006, ApJS, 172, 239
Mei, S., et al. 2006, ApJ, 639, 81
Mellier, Y. 1999, ARA&A, 37, 127
Mobasher, B., et al. 2007, ApJS, 172, 117
Murayama, T., et al. 2007, ApJS, 172, 523
Park, Y., et al. 2004, ApJ, 600, L155
Peebles, J. E. 2002, in ASP Conf. Ser. 283, A New Era in Cosmology, ed. N. Metcalfe & T. Shanks (San Francisco: ASP), 351
Refregier, A. 2003, ARA&A, 41, 645
Renzini, A. 2006, ARA&A, 44, 141
Rhodes, J. R., et al. 2007, ApJS, 172, 203
Rix, H.-W., et al. 2004, ApJS, 152, 163
Sanders, D. B., et al. 2007, ApJS, 172, 86
Scarlata, C., et al. 2007, ApJS, 172, 406
Schinnerer, A., et al. 2007, ApJS, 172, 46
Scoville, N., et al. 2007a, ApJS, 172, 38
———. 2007b, ApJS, 172, 150
Shapley, A., Steidel, C. C., Adelberger, K. L., Dickinson, M., Giavalisco, M., & Pettini, M. 2001, ApJ, 562, 95
Smail, I., Ivison, R. J., Blain, A. W., & Kneib, J.-P. 2002, MNRAS, 331, 495
Smith, G. 2002, MNRAS, 330, 1
Springel, V., et al. 2005, Nature, 435, 629
Steidel, C. C., Shapley, A. E., Pettini, M., Adelberger, K. L., Erb, D. K., Reddy, N. A., & Hunt, M. P. 2004, ApJ, 604, 534
Taniguchi, Y., et al. 2007, ApJS, 172, 9
Williams, R. E., et al. 1996, AJ, 112, 1335
———. 2000, AJ, 120, 2735
Zamojski, M. A., et al. 2007, ApJS, 172, 468